ResearchGate

See discussions, stats, and author profiles for this publication at: https://www.researchgate.net/publication/7059551

Enzyme Activity to Augment the Characterization of Tethered Bilayer Membranes

ARTICLE *in* THE JOURNAL OF PHYSICAL CHEMISTRY B · JULY 2006

Impact Factor: 3.3 · DOI: 10.1021/jp0616516 · Source: PubMed

CITATIONS
49

READS
22

6 AUTHORS, INCLUDING:

Gintaras Valincius
Vilnius University
82 PUBLICATIONS **1,086** CITATIONS
SEE PROFILE

Duncan J. McGillivray
University of Auckland
39 PUBLICATIONS **828** CITATIONS
SEE PROFILE

David J Vanderah
Institute for Bioscience and Biotechnology R…
90 PUBLICATIONS **1,846** CITATIONS
SEE PROFILE

Mathias Lösche
Carnegie Mellon University
146 PUBLICATIONS **3,923** CITATIONS
SEE PROFILE

Available from: David J Vanderah
Retrieved on: 31 January 2016

THE JOURNAL OF PHYSICAL CHEMISTRY B LETTERS

2006, *110,* 10213−10216
Published on Web 05/10/2006

Enzyme Activity to Augment the Characterization of Tethered Bilayer Membranes

Gintaras Valincius,[†] Duncan J. McGillivray,[‡,§] Wilma Febo-Ayala,[||,⊥] David J. Vanderah,*[,||] John J. Kasianowicz,[#] and Mathias Lösche[‡,§]

Institute of Biochemistry, Mokslininku 12, LT-08662 Vilnius, Lithuania, National Institute of Standards and Technology (NIST) Center for Neutron Research (NCNR), Gaithersburg, Maryland 20899, Physics Department, Carnegie Mellon University, Pittsburgh, Pennsylvania 15213, NIST Biochemical Science Division, Gaithersburg, Maryland 20899, and NIST Semiconductor Electronics Division, Gaithersburg, Maryland 20899

Received: March 16, 2006; In Final Form: April 20, 2006

The rate of Ca^{2+}-triggered phospholipase A_2 (PLA_2) degradation of tethered bilayer membranes (tBLMs), composed of a synthetic lipid, β-mercaptoethanol, and palmitoyloleoylphosphatidylcholine (POPC), is ~80 times greater than for those prepared with diphytanoylphosphatidylcholine (DPhyPC). Electrochemical impedance spectroscopy (EIS) and neutron reflectivity (NR) data indicate complete, water-free tBLMs that exhibit near ideal capacitive behavior and the presence of a water reservoir in the bilayer subspace proximal to the substrate (Au) surface for both tBLMs. Together these data indicate that the POPC and the DPhyPC tBLMs are structurally similar along the surface normal but markedly different at the outer leaflet/solution interface and that PLA_2 is a sensitive probe of short length scale structural differences not revealed by EIS and NR.

Introduction

Tethered bilayer membranes (tBLMs) on gold substrates are biomimetic systems that provide a (phospho)lipid matrix for the incorporation of membrane proteins on a conductive solid support. These systems can serve as a functional link between membrane constituents and an electrode which might be exploited in, e.g., biosensor applications.[1] Solid supported bilayers can be easily deposited on surfaces by vesicle fusion.[2] However, the functional reconstitution of protein within supported membranes requires the membrane to be spatially separated from the substrate. This decoupling maintains lateral fluidity and provides a solvent compartment adjacent to the solid surface that may accommodate solvent-exposed protein domains and serve as an ionic reservoir.[1,3] In this work, the decoupling is achieved by a 1-thiahexa(ethylene oxide) (THEO) segment of a synthetic lipid, 20-tetradecyloxy-3,6,9,12,15,18,22-heptaoxahexatricontane-1-thiol (WC14, see Figure 1).[4] tBLM preparation is initiated with the formation of a mixed self-assembled monolayer (SAM) of WC14 and β-mercaptoethanol (β-ME). It is completed by the addition of lipids,[1,5−8] in our case, the structurally different phosphatidylcholines, (PCs) 1-palmitoyl-2-oleoyl-*sn*-glycero-3-phosphocholine (POPC) or 1,2-diphytanoyl-*sn*-glycero-3-phosphocholine (DPhyPC). Surface backfilling between grafted THEO segments with the hydrophilic β-ME provides for space, by virtue of the different molecular lengths, to incorporate water in the tBLM tether region (see sketch in Figure 1). We thus create a suitable hydrophilic environment for both ends of transmembrane proteins.

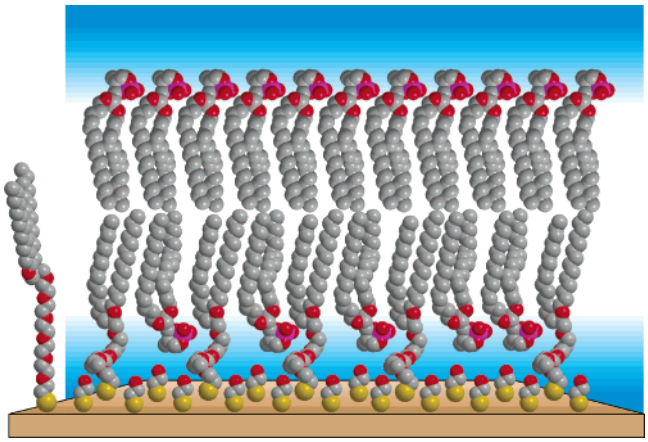

Figure 1. Molecular model of WC14 (leftmost) and illustration of a tBLM (right), such as those investigated here. On the left, the tether in WC14 is depicted in the extended all-trans conformation to show the oxygen atoms in the THEO segment. In the tBLM, on the other hand, WC14 is depicted as less ordered, consistent with reflection−absorption infrared spectroscopy data.[18]

Recent studies have indicated that tBLMs are good matrixes for the reconstitution of transmembrane protein ion channels,[1,5−8] transporters such as H^+-ATPase,[5] Na^+- and K^+-ATPase,[8] and transmembrane receptors.[7] The incorporation of other pore-forming channels such as α-hemolysin extends the potential of solid-supported tBLMs as a technology platform to include ion channel-switch biosensors,[1] single molecule stochastic sensors,[9] and DNA sequencing devices.[10]

* Corresponding author. E-mail: david.vanderah@nist.gov.
† Institute of Biochemistry.
‡ NIST Center for Neutron Research.
§ Carnegie Mellon University.
|| NIST Biochemical Science Division.
⊥ Current address: Department of Chemistry, Purdue University, West Lafayette, IN 47907.
NIST Semiconductor Electronics Division.

10.1021/jp0616516 CCC: $33.50 © 2006 American Chemical Society

Although the express purpose of tBLM preparation is to prepare a biologically relevant matrix for the study of membrane processes, such as the incorporation of peripheral and integral membrane proteins, we show here that interaction of proteins, such as phospholipase A_2 (PLA_2), with the membrane may also be judiciously used for tBLM molecular-level characterization. PLA_2 cleaves the acyl-ester bond at the *sn*-2 position of glycerophospholipid aggregates in a Ca^{2+}-dependent manner. Its activity depends on the collective organization of the substrate and is sensitive to the physical state (e.g., phase equilibrium, lateral packing, etc.) of the aggregates, as has been shown for vesicles,[11] supported bilayers,[12] hybrid bilayer membranes,[13,14] and monolayers at the air−water interface.[15,16] In this report, we use the sensitivity of PLA_2 as a probe of the physical properties of tBLMs to augment the characterization of tBLMs using electrochemical impedance spectroscopy (EIS) and neutron reflectivity (NR) measurements.

Experimental Section[17]

Mixed SAMs were prepared by exposure of magnetron-sputtered Au films (∼2000 Å in EIS, ∼200 Å in NR experiments) to solutions of WC14:β-ME (3:7 mol:mol, 0.2 mM total concentration) in 99.5% ethanol for >12 h. The tBLMs were subsequently completed by incubating the mixed SAM surface with 20 mM ethanolic solutions of POPC or DPhyPC followed by rapid solvent exchange[1,7] with an aqueous solution of 0.1 M KCl, 0.01 M 2-amino-2-hydroxymethyl-1,3-propanediol (Tris-HCl, Sigma), pH 7.8.[18] The EIS measurements and data analysis were carried out as described earlier.[19] Neutron reflectivity measurements were performed on the Advanced Neutron Diffractometer/Reflectometer (AND/R)[20] at the NIST Center for Neutron Research (NCNR) and modeled using the Parratt box model formalism[21] with software developed at the NCNR.[22] *Apis mellifera* venom PLA_2 (EC 3.1.1.4) was purchased from Sigma as a lyophilized salt-free powder (1474 units/mg) and used without further purification.

Results and Discussion

The structures of the tBLMs as characterized by NR are shown in Figure 2 before and after incubation with PLA_2. Molecularly-resolved material density profiles along the surface normal, z, were determined by modeling the data in terms of neutron scattering length density (nSLD) profiles, $\rho_n(z)$, for various solvent (H_2O/D_2O) contrasts.[18] Among other structural parameters, the hydration of the membrane interface proximal to the metal substrate can thus be precisely determined. Parameters and confidence levels are compiled in Table 1. Both POPC and DPhyPC tBLMs incorporate complete, water-free bilayer structures. Distinct ρ_n profiles near $z \sim 20$ Å for the different water contrasts show significant hydration of the membrane subspaces, which are ∼12 and ∼15 Å thick for the POPC and the DPhyPC tBLMs, respectively. The hydrophobic leaflets have low nSLD, consistent with condensed alkane phases.[23] The thickness of the alkane layer, L_{alkane}, was found to be ∼31 and ∼35 Å for the DPhyPC and the POPC tBLMs, respectively. However, their phase states, L_α or L_β, and thus the local order of the bilayer surface, cannot be determined from these data, as $|\rho_n|$ of protonated alkanes is small. As a consequence, the variations in ρ_n expected for phase-state dependent chain packing differences are below the precision of the measurement.

Figure 3, panels A and B, shows Nyquist plots, Im Y/ω vs Re Y/ω, from the EIS spectra for the POPC and DPhyPC tBLMs, and the tethered mixed SAM, where Y is the electrode admittance and ω is the angular frequency. Parts of the EIS plots are semicircular and indicate near-ideal behavior for both tBLMs (Figure 3A). The diameter of the semicircle is proportional to the magnitude of the SAM or tBLM capacitance. As seen from Figure 3B, the capacitance of the SAM precursor decreases significantly upon bilayer formation, indicating an increase of the dielectric layer thickness. The best fits to the experimental curves are obtained using the electrical equivalent model shown in the inset of Figure 3A.[24] For SAMs prepared from WC14:β-ME (3:7 mol:mol) solutions, we obtained mean values for the specific capacitances of 0.65(3) and 0.59(3) μF/cm^2 for the POPC and DPhyPC tBLMs, respectively.[25] Typically, these values were stable for 4−12 h. They are comparable to the capacitance of (unsupported) black lipid membranes,[26−28] as well as to tBLM capacitances reported by others.[1,3,6,29] Notably, despite smaller L_{alkane} values (Table 1), the DPhyPC tBLMs exhibited consistently lower capacitances than POPC tBLMs, indicating lower dielectric permeability of its hydrophobic alkane region. When the capacitances are related to the NR thickness data, the dielectric constants of the tBLM alkane layers in the tBLMs were found to be 2.08(11) and 2.54(12) for DPhyPC and POPC, respectively. These data indicate higher disorder and/or hydration of the alkane region within the POPC tBLM.

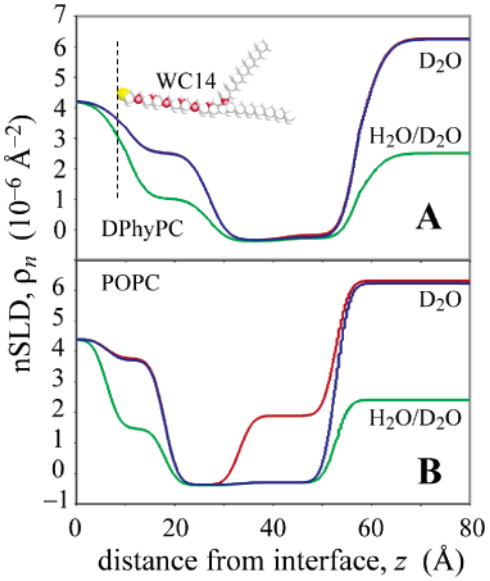

Figure 2. nSLD profiles of the surface architecture starting at the Au surface ($z = 0$ Å) of a DPhyPC (A) and a POPC (B) tBLM. Different solvent contrasts are shown in green (H_2O/D_2O mixtures) and blue or red (D_2O). Profiles in blue/red were obtained before/after PLA_2 incubation. Note that for DPhyPC the red nSLD profile retraces the blue profile almost perfectly. The DPhyPC panel includes a scaled model of WC14.

TABLE 1: Parameters from Neutron Reflectivity Models for the POPC and DPhyPC tBLMs

sample	spacer thickness, L_{spacer} (Å)	vol. fraction of water in spacer	alkane layer thickness, L_{alkane} (Å)	vol. fraction of water in alkane layer[a]
POPC	12(1)	0.59(5)	35(1)	0.01(5)
−after PLA_2	12(1)	0.59(5)	inner: 15 (1)	0.01(5)
			outer: 20 (1)	0.33(2)
DPhyPC	15(1)	0.45(5)	31(1)	0.02(5)
−after PLA_2	15(1)	0.45(5)	31(1)	0.03(5)

[a] This is interpreted as the upper limit of water that fills residual defects in the bilayer rather than the density of water molecules "dissolved" in the alkane phase.

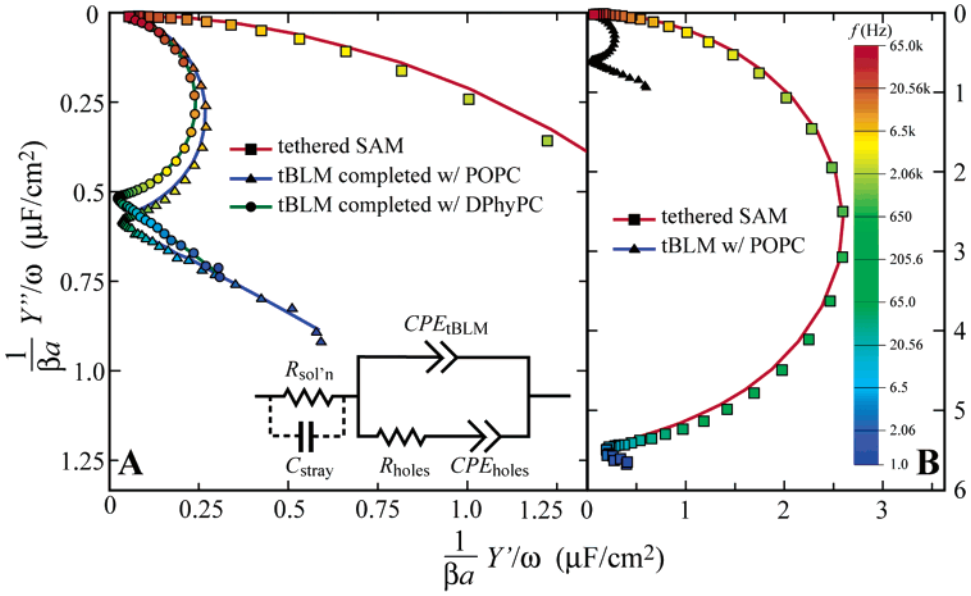

Figure 3. Nyquist plots of Y/ω for a POPC and a DPhyPC tBLM and a WC14:β-ME (3:7 mol:mol) precursor SAM. (A) expanded view and (B) condensed view. The data points are color-coded for frequency according to the scale shown on the right and have been modeled (solid lines) according to the equivalent circuit shown in A. The data were normalized with respect to the geometric surface area (a) and roughness factor (β).

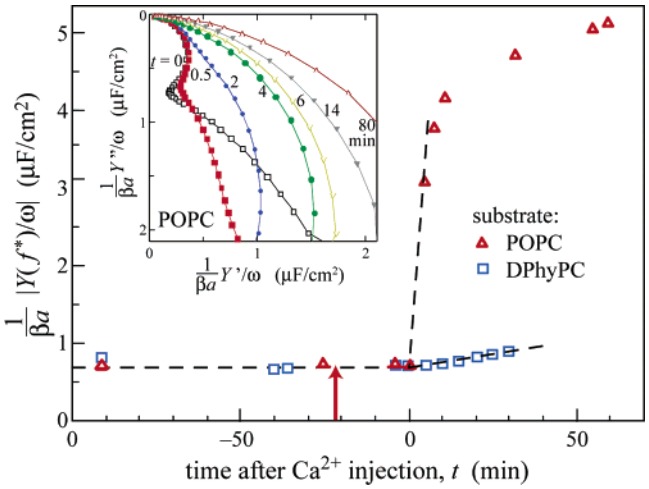

Figure 4. Temporal development of the complex capacitance magnitude $|Y/\omega|_{f^* = 206\ \mathrm{Hz}}$ for a POPC and a DPhyPC tBLM before and after PLA_2 injection (~2.0 μM; red arrow). Ca^{2+} (5 mM) was injected at $t = 0$. The data were normalized with respect to the geometric surface area (a) and roughness factor (β). Broken lines are guides for the eye. The inset shows the Nyquist plots for the POPC tBLM from which the data in the main panel were derived.

Under the Ca^{2+}-mediated action of PLA_2, the tBLMs undergo enzymatic degradation, as the resulting lysolipids and fatty acids exhibit a propensity for the formation of nonlamellar phases[12] and thus destabilize the planar lipid assembly. Because the EIS spectra indicate near-ideal capacitive behavior, one may monitor the PLA_2-induced tBLM degradation at a single EIS frequency f^* ($= \omega^*/2\pi$) at which the impedance is mostly determined by the bilayer capacitance. The data point closest to the Y''/ω axis in the Nyquist plot, where $Y'/\omega \rightarrow 0$, is most appropriate for such an analysis. In the sample shown in Figure 3B, this occurs at f^* ~206 Hz. Variations of $|Y/\omega|$ measured at f^* during the interaction of PLA_2 with the POPC and DPhyPC tBLMs are shown in Figure 4. For both lipids, $|Y/\omega|$ remains virtually constant after PLA_2 injection. Subsequent injection of Ca^{2+} triggers an increase of $|Y/\omega|$ that occurs within minutes for both tBLMs. For the POPC tBLMs, the increase levels off as $|Y/\omega|$ reaches a value characteristic of the precursor SAM (typically, $|Y(t \rightarrow \infty)/\omega| = 5-7\ \mu\mathrm{F/cm^2}$). For the DPhyPC tBLMs, the initial reaction rate is ~ 80 fold slower (Figure 4), as determined from the initial slopes of $|Y(t)/\omega|$ after Ca^{2+} injection. Preliminary data show that the rate of the Ca^{2+}-triggered increase in $|Y(t)/\omega|$ is proportional to the concentrations of PLA_2 and Ca^{2+}.

The structural effects of the PLA_2 activity[30] on the tBLMs are seen in the NR data (Table 1). After PLA_2 injection, the water volume fraction in the outer leaflet of the POPC tBLM increases drastically, whereas the inner leaflet is left intact. This has been labeled the "scooting mode" of the PLA_2 action,[31] where it was observed that the irreversibly bound enzyme hydrolyzes all of the substrate in the outer leaflet of a vesicle bilayer, while completely retaining the physical integrity of the inner leaflet.

The high specificity of PLA_2 enzymatic activity indicates short length scale structural differences in the outer leaflet/solution interfaces for the two tBLMs. Because of different molecular constitutions of the hydrophobic segments in POPC and DPhyPC, differences in the short-range order, deriving from, e.g., different local defect densities or different phase states, are expected.[32] Such subtle differences are below the detection limits of both NR and EIS. One possible cause of the lower PLA_2 turnover rate at tBLMs completed with DPhyPC is a more uniform, "space-filling" organization of the outer leaflet than with POPC. The packing of the branched phytanoyl chains has been described as like "two combs inserting into each other".[33] Such packing would result in higher free transfer energies for an individual lipid molecule from the bilayer to the reaction site within the enzyme. A second, distinct factor in the difference in turnover rates may be that the unsaturated chains in POPC lead to a higher density of membrane packing defects than for DPhyPC. PLA_2 activity has been shown to be enhanced by local defects, such as microdomains, disclinations, collapse sites, or pinholes.[12,32]

Whatever the cause, PLA_2 interrogates the outer leaflet over a length scale that exposes the structural differences of these tBLMs. In that sense, PLA_2 acts as a sensitive amplifier of the physical properties of the phospholipid membrane that are not resolved by other surface metrologies. The results reported here thus show that enzymatic activity can be a useful tool for bilayer

characterization. The observations have practical significance. Because the enzymatic activity is concentration dependent, tBLM-based devices can be developed to monitor for secretory PLA_2, analogous to approaches described earlier,[34] but much simpler to use than the mercury electrode-based techniques reported there. As phospholipases comprise a large class of secretory toxins, the quest for fast pharmacological screening for inhibitors might also provide opportunities for the application of tBLM-based sensor devices.

Acknowledgment. Helpful discussions with John T. Elliott are gratefully acknowledged. This work was supported by the NSF (CTS-0555201 and 0457148), the NIH (1 RO 1 RR14182), the Volkswagen foundation (I/77709), the European Union (NMP4-CT-2003-505211), the NIST *Single Molecule Manipulation and Measurement Program*, and The Regents of the University of California. W.F.-A. (then at the University of Puerto Rico at Cayey) was supported by the NIST's Chemical Science and Technology summer undergraduate research fellowship (SURF) 1999 and 2000.

Supporting Information Available: A simplified synthesis scheme for WC14 and EIS model parameters for the data shown in Figure 3. This material is available free of charge via the Internet at http://pubs.acs.org.

References and Notes

(1) Cornell, B. A.; Braach-Maksvytis, V. L. B.; King, L. B.; Osman, P. D. J.; Raguse, B.; Wieczorek, L.; Pace, R. J. *Nature* **1997**, *387*, 580.

(2) Tamm, L. K.; McConnell, H. M. *Biophys. J.* **1985**, *47*, 105.

(3) Williams, L. M.; Evans, S. D.; Flynn, T. M.; Marsh, A.; Knowles, P. F.; Bushby, R. J.; Boden, N. *Langmuir* **1997**, *13*, 751.

(4) See Supporting Information for a simplified synthesis scheme; full details will be published elsewhere.[18]

(5) Bunjes, N.; Schmidt, E. K.; Jonczyk, A.; Rippmann, F.; Beyer, D.; Ringsdorf, H.; Gräber, P.; Knoll, W.; Naumann, R. *Langmuir* **1997**, *13*, 6188.

(6) Krishna, G.; Schulte, J.; Cornell, B. A.; Pace, R. J.; Osman, P. D. *Langmuir* **2003**, *19*, 2294.

(7) Stora, T.; Lakey, J. H.; Vogel, H. *Angew. Chem., Int. Ed. Engl.* **1999**, *38*, 389.

(8) Zebrowska, A.; Krysinski, P. *Langmuir* **2004**, *20*, 11127.

(9) Bezrukov, S. M.; Kasianowicz, J. J. *Phys. Rev. Lett.* **1993**, *70*, 2352.

(10) Kasianowicz, J. J.; Brandin, E.; Branton, D.; Deamer, D. W. *Proc. Natl. Acad. Sci. U.S.A.* **1996**, *93*, 13770.

(11) Lehtonen, J. Y. A.; Kinnunen, P. K. J. *Biophys. J.* **1995**, *68*, 1888.

(12) Jörgensen, K.; Davidsen, J.; Mouritsen, O. G. *FEBS Lett.* **2002**, *531*, 23.

(13) Elliott, J. T.; Meuse, C. W.; Krueger, S.; J. T. Woodward; Petrall-Mallow, T.; Plant, A. L. In *Biomolecular Films. Design, Function and Applications*; Rusling, J., Ed.; Marcel Dekker: New York, 2003; p 99.

(14) Stelzle, M.; Weissmüller, G.; Sackmann, E. *J. Phys. Chem.* **1993**, *97*, 2974.

(15) Reichert, A.; Ringsdorf, H.; Wagenknecht, A. *Biochim. Biophys. Acta* **1992**, *1106*, 178.

(16) Grainger, D. W.; Reichert, A.; Ringsdorf, H.; Salesse, C. *Biochim. Biophys. Acta* **1990**, *1023*, 365.

(17) Certain commercial materials, instruments, and equipment are identified in this manuscript in order to specify the experimental procedure as completely as possible. In no case does such identification imply a recommendation or endorsement by the National Institute of Standards and Technology nor does it imply that the materials, instruments, or equipment identified is necessarily the best available for the purpose.

(18) McGillivray, D. J.; Valincius, G.; Vanderah, D. J.; Febo-Ayala, W.; Woodward, J. T.; Kasianowicz, J. J.; Lösche, M. **2006**, in preparation.

(19) Vanderah, D. J.; Gates, R. S.; Silin, V.; Zeiger, D. N.; Woodward, J. T.; Meuse, C. W.; Valincius, G.; Nickel, B. *Langmuir* **2003**, *19*, 2612.

(20) Dura, J. A.; Pierce, D.; Majkrzak, C. F.; Maliszewskyj, N.; McGillivray, D. J.; Mihailescu, M.; Perez-Salas, U. A.; Worcester, D.; Lösche, M.; White, S. H. *Rev. Sci. Instrum.* **2006**, to be submitted.

(21) Parratt, L. G. *Phys. Rev.* **1954**, *95*, 359.

(22) Kienzle, P. A.; Doucet, M.; McGillivray, D. J.; O'Donovan, K. V.; Berk, N. F.; Majkrzak, C. F. http://www.ncnr.nist.gov/reflpak/garefl.html.2000−2006.

(23) $\rho_n \sim -0.5 \times 10^{-6}$ Å^{-2} is expected for a condensed phase at the lower limit of alkane packing density; the NR models suggest that the hydrophobic leaflets are only slightly above this physical limit.

(24) This model gives a better fit to the EIS data than models used earlier.[13,35,36] Its physical basis will be discussed in a forthcoming publication.

(25) Specific capacitances C were obtained from the modeled constant phase elements, CPE_{tBLM}, by accounting for the geometric surface area of the electrode ($a \sim 0.32$ cm^2) and the roughness factor of the gold surface ($\beta \sim 1.49$): $C \approx CPE_{tBLM}/(a \cdot \beta)$. β was determined in accordance with ref 37.

(26) Mueller, P.; Rudin, D. O.; Tien, H. T.; Wescott, W. C. *Nature* **1962**, *194*, 979.

(27) Redwood, W. R.; Pfeiffer, F. R.; Weisbach, J. A.; Thompson, T. E. *Biochim. Biophys. Acta* **1971**, *233*, 1.

(28) Schuster, B.; Weigert, S.; Pum, D.; Sára, M.; Sleytr, U. B. *Langmuir* **2003**, *19*, 2392.

(29) Römer, W.; Lam, Y. H.; Fischer, D.; Watts, A.; Fischer, W. B.; Göring, P.; Wehrspohn, R. B.; Gösele, U.; Steinem, C. *J. Am. Chem. Soc.* **2004**, *126*, 16267.

(30) PLA_2 hydrolysis takes place at an internal active center ∼15 Å from the surface of the enzyme.[38,39] Enzymatic degradation of the outer leaflet requires: (a) initial binding of the PLA_2 to the bilayer, (b) extraction of a PC molecule from the leaflet, (c) transport of the extracted lipid to the active center, and (d) release of the products.

(31) Jain, M. K.; Gelb, M. H. Phospholipase-A_2-catalyzed hydrolysis of Vesicles—Uses of interfacial catalysis in the scooting mode. In *Methods In Enzymology*; Academic Press: New York, 1991; Vol. 197; p 112.

(32) Hönger, T.; Jörgensen, K.; Biltonen, R. L.; Mouritsen, O. G. *Biochemistry* **1996**, *35*, 9003.

(33) Hung, W. C.; Chen, F. Y.; Huang, H. W. *Biochim. Biophys. Acta* **2000**, *1467*, 198.

(34) Chen, S.; Abruña, H. D. *Langmuir* **1997**, *13*, 5969.

(35) Raguse, B.; Braach-Maksvytis, V. L. B.; Cornell, B. A.; King, L. B.; Osman, P. D. J.; Pace, R. J.; Wieczorek, L. *Langmuir* **1998**, *14*, 648.

(36) Jeuken, L. J. C.; Connell, S. D.; Nurnabi, M.; O'Reilly, J.; Henderson, P. J. F.; Evans, S. D.; Bushby, R. J. *Langmuir* **2005**, *21*, 1481.

(37) Burstein, R. K. *Elektrokhimiya* **1967**, *3*, 349.

(38) Jain, M. K.; Yu, B. Z.; Rogers, J.; Ranadive, G. N.; Berg, O. G. *Biochemistry* **1991**, *30*, 7306.

(39) Scott, D. L.; White, S. P.; Otwinowski, Z.; Yuan, W.; Gelb, M. H.; Sigler, P. B. *Science* **1990**, *250*, 1541.